Published in final edited form as:
Hum Brain Mapp. 2010 September ; 31(9): 1339–1347. doi:10.1002/hbm.20934.

Hippocampal Atrophy Patterns in Mild Cognitive Impairment and Alzheimer's Disease

Susanne G. Mueller[1], **Norbert Schuff**[1], **Kristine Yaffe**[2], **Catherine Madison**[3], **Bruce Miller**[4], and **Michael W. Weiner**[1,*]

[1]Center for Imaging of Neurodegenerative Diseases, Department of Veterans Affairs Medical Center, San Francisco, California

[2]Memory Disorders Clinic, Department of Veterans Affairs Medical Center, San Francisco, California

[3]Memory Clinic, California Pacific Medical Center, San Francisco, California

[4]Memory and Aging Center, UCSF, San Francisco, California

Abstract

Background—Histopathological studies and animal models suggest that hippocampal subfields may be differently affected by aging, Alzheimer's disease (AD), and other diseases. High-resolution images at 4 Tesla depict details of the internal structure of the hippocampus allowing for in vivo volumetry of different subfields. The aims of this study were as follows: (1) to determine patterns of volume loss in hippocampal subfields in normal aging, AD, and amnestic mild cognitive impairment (MCI). (2) To determine if measurements of hippocampal subfields provide advantages over total hippocampal volume for differentiation between groups.

Methods—Ninety-one subjects (53 controls (mean age: 69.3 ± 7.3), 20 MCI (mean age: 73.6 ± 7.1), and 18 AD (mean age: 69.1 ± 9.5) were studied with a high-resolution T2 weighted imaging sequence aimed at the hippocampus. Entorhinal cortex (ERC), subiculum, CA1, CA1–CA2 transition zone (CA1-2), CA3 & dentate gyrus (CA3&DG) were manually marked in the anterior third of the hippocampal body. Hippocampal volume was obtained from the Freesurfer and manually edited.

Results—Compared to controls, AD had smaller volumes of ERC, subiculum, CA1, CA1-2, and total hippocampal volumes. MCI had smaller CA1-2 volumes. Discriminant analysis and power analysis showed that CA1-2 was superior to total hippocampal volume for distinction between controls and MCI.

Conclusion—The patterns of subfield atrophy in AD and MCI were consistent with patterns of neuronal cell loss/reduced synaptic density described by histopathology. These preliminary findings suggest that hippocampal subfield volumetry might be a better measure for diagnosis of early AD and for detection of other disease effects than measurement of total hippocampus.

Keywords

hippocampal subfields; Alzheimer's disease; manual parcellation; MRI

*Correspondence to: Michael W. Weiner, Center for Imaging of Neurodegenerative Diseases, Department of Veterans Affairs (DVA) Medical Center, Clement Street 4150, San Francisco, CA, 94121. michael.weiner@ucsf.edu.

Additional Supporting Information may be found in the online version of this article.

INTRODUCTION

Memory impairment is a characteristic early sign of Alzheimer's Disease (AD) and atrophy of the memory related medial temporal structures, particularly the hippocampal formation, is one of its earliest macroscopical hallmarks and has been consistently reported in autopsy and neuroimaging studies. However, the hippocampus is not a homogeneous structure but consists of several subfields with distinct histological characteristics: the subiculum, the three cornu ammonis sectors (CA1–3), and the dentate gyrus. Although these subfields are functionally tightly interconnected [Duvernoy, 2005], there is evidence for a functional specialization, i.e. different hippocampal subfields are responsible for the processing of different aspects of the memory content, e.g. CA3 for spatial information and CA1 for temporal information [Kesner and Hopkins, 2006; Rolls and Kesner, 2006]. There is also evidence from animal models and histopathological studies that different disease processes affect subfields differently, e.g. stress affects predominantly the dentate gyrus while AD typically shows the most prominent neuron loss in CA1 [Lucassen et al., 2006; West et al., 1994, 2004]. Therefore, measurements of subfield volumes might yield a better distinction between different disease processes affecting the hippocampus than measurements of the total hippocampal volume.

However, measuring hippocampal subfields in vivo with MRI requires that details of the internal structure of the hippocampal formation as additional anatomical landmarks for subfield assignment can be depicted. On a clinical 1.5-T magnet the sensitivity of the MR signal is usually too low to obtain sufficient resolution to identify individual subfields without the application of sophisticated, often lengthy imaging protocols. Nonetheless, there have been several attempts to either directly visualize age and AD-related structural and perfusion changes in hippocampal subfields at 1.5 T using specially designed acquisition schemes [Adachi et al., 2003; Small et al., 2004] or to use sophisticated imaging processing techniques like unfolding, surface mapping, or shape deformation to make indirect inferences about localized volume loss of the hippocampal formation in AD and other disease processes [Apostolova et al., 2006a, b; Csernansky et al., 2005; Wang et al., 2006]. Recent advancements with high field MRI (3–4 T) resulting in improved gray/white matter contrast due to the increased signal sensitivity at high fields, additional magnetization transfer effects and T1 weighting, allow to acquire excellent anatomical images at sub-millimeter resolution within a few minutes [Mueller et al., 2007; Zeineh et al., 2000].

Using such a high-resolution protocol on a 4-T MR magnet, we developed a manual marking scheme based on the internal features and other hippocampal landmarks to study the effects of healthy aging on different subfields. We found that age-related volume losses of the hippocampus were due to volume loss in the CA1 sector [Mueller et al., 2007]. In this study, the same protocol is used to identify regions of hippocampal volume loss in subjects diagnosed with amnestic mild cognitive impairment (MCI) who have a heightened risk to develop AD and subjects diagnosed with AD. The specific aims of this study were the following: (1) To determine if patterns of volume loss in hippocampal subfields in patients suffering from AD and MCI are different from normal aging. Based on the findings reported in histopathological studies we expected to find the most prominent AD related volume losses in CA1 [West et al., 1994]. (2) To test if the measurement of hippocampal subfields allows for a better discrimination between controls and patients suffering from MCI or AD than measurements of total hippocampal volume loss.

METHODS

Study Population

A total of 96 subjects were evaluated for the study. Five had to be excluded (cf. postprocessing) so that a total of 91 participated in this study (mean age 70.2 ± 7.8, range: 51–86 years, female/

male (f/m) 33/58). Fifty-three were healthy control subjects (mean age: 69.5 ± 7.3, f/m: 21/31, mean MMSE: 29.3 ± 1.1, range: 25–30) recruited from the community with flyers and advertisements in local newspapers. Eleven subjects of this group were part of a study about normal aging reported in a previous publication [Mueller et al., 2007]. Exclusion criteria included any poorly controlled medical illness and/or use of medication or recreational drugs affecting brain function or history of other neurological disease. Normal cognitive functioning was assessed by a battery of neuropsychological tests (mini mental state examination, California Verbal Learning Test (short form), Rey-Osterrieth complex figure, Verbal Fluency, Wechsler Adult Intelligence Score (digit symbol, digit span); emotional state with Geriatric Depression Scale and functioning in daily living with Functional Activities Questionnaire). Eighteen subjects (mean age: 69.1 ± 9.6, f/m: 6/12, mean MMSE: 21.6 ± 5.1, range: 11–29) who had been diagnosed with AD according to the criteria of the National Institute of Neurological and Communication Disorders and Stroke/Alzheimer's Disease and Related Disorders Association (NINDS-ADRDA), and 20 subjects (mean age: 73.5 ± 7.1, f/m: 6/14, mean MMSE: 28.0 ± 2.1, range: 25–30) meeting the criteria for amnestic MCI according to Petersen et al. [1999] were referred from collaborating Memory Clinics (UCSF, VA Medical Center, CPMC San Francisco). The three groups differed regarding MMSE score (Kruskal–Wallis, $P < 0.001$), with the AD group having lower scores than the MCI group and controls (Mann–Whitney, $P < 0.05$) and the MCI group having lower scores than controls (Mann–Whithey, $P < 0.05$). Their age was not significantly different (ANOVA, $F(2,88) = 2.4$, $P = 0.09$). The study was approved by the committees of human research at the University of California, San Francisco (UCSF) and VA Medical Center San Francisco. Written informed consent was obtained from all subjects or their legal representatives according to the Declaration of Helsinki.

MRI Acquisition

The following sequences were acquired on a Bruker MedSpec 4T system equipped with a USA instruments eight-channel array coil: (1) For subfield measurement, a high-resolution T2 weighted fast spin echo sequence (TR/TE: 3,500/19 ms, 0.4 mm × 0.4 mm in plane resolution, 2 mm slice thickness, 24 interleaved slices without gap, acquisition time 5:30 min [Thomas et al., 2004; De Vita et al., 2003], angulated perpendicular to the long axis of the hippocampal formation. (2) For measurement of total hippocampal volume a volumetric T1-weighted gradient echo MRI (MPRAGE) TR/TE/TI = 2,300/3/950 ms, 1.0 mm × 1.0 mm × 1.0 mm resolution. (3) For determination of the intracranial volume (ICV), a T2-weighted turbospin echo sequence, TR/TE: 8,390/70 ms, 0.9 mm × 0.9 mm × 3 mm resolution, 54 slices.

Postprocessing

The method used for subfield marking has been described in detail previously [Mueller et al., 2007]. To summarize the procedure briefly: The high-resolution images were resampled to obtain a left and a right hippocampal image to ensure that the hippocampal cross-section used for marking was perpendicular to the long axis of the hippocampus on each side. The marking scheme depends on anatomical landmarks, particularly on a hypointense line which probably represents myelinated fibers in the strata moleculare and lacunosum [Eriksson et al., 2008] (cf. Figs. 1 and 2). Five subjects (3 AD, 1 MCI, and 1 control) fulfilling the inclusion criteria and thus selected for the project could not be marked because the internal structure could not be sufficiently visualized and had to be excluded. The distance between this hypointense line and the outer surface of the hippocampus provides a direct measure of the subfield thickness at this point. Although the sequence used in this study provides superior resolution, it does not allow distinguishing details on the resolution of a histological preparation. Therefore, a set of arbitrarily defined hippocampal landmarks was used to assign different regions to different subfields. We do not claim that this subfield assignment actually corresponds to the histological subfields but merely that it provides a good and reproducible approximation. The marking

started on the first slice on which the head of the hippocampus was no longer visible. On this slice, the hippocampal subfields, subiculum, and ERC were marked manually. In addition, the ERC was marked on the two slices anterior to this starting slice and the subiculum and the hippocampal subfields were marked on the two slices posterior to it. Altogether, the hippocampus is marked on about 1 cm in the anterior third of its body, i.e., disease effects in the head or tail region will be missed. The most medial point of the temporal cortex was chosen as medial border of the ERC, and the end of the collateral sulcus was chosen as lateral border. The CA1/subiculum border was determined by drawing a line perpendicular to the edge of the subiculum touching the medial border of the hippocampus. CA2 is the smallest hippocampal subfield and its visualization requires special stains even in histological specimens. Furthermore, there are no macroscopic hippocampal landmarks for CA2 which help to identify it in the high-resolution image. Therefore, the CA1/CA2 border was determined by dividing the line along the longest diameter of the hippocampus by two and drawing a line perpendicular to this line. A region supposed to represent mainly CA2 was marked in a square-like manner, i.e., its height at the CA1/CA2 boundary also determined its length while its overall shape was determined by the course of the outer boundary of the hippocampus and the hypointense line. Pathological processes affecting CA2 will result in a thinning of the subfield in all directions and marking CA2 in a square-like manner should capture this phenomenon. However, the volume of this label is relatively small thus rendering it sensitive to small marking inaccuracies (cf. Table I). Although the position of CA2 showed good correspondence with the localization of CA2 in histological preparations, its position relatively to the fimbriae, which can be used as a macroscopic landmark of CA3 in this section of the hippocampus (cf Fig. 1b), varies slightly depending on the shape of the hippocampus. Furthermore, the volume of this subfield is influenced by the width of the dorsal CA1 and it is likely to have some overlap with the dorsomedial part of CA1. Because of this, we expect that volume changes in this sector can result from changes in both subfields. To reflect this “contamination” by CA1, the region was named CA1-2 transition zone (CA1-2 transition) rather than CA2. The remainder of the hippocampal formation consisting of CA3 and dentate gyrus was marked as one region (CA3&DG) because there were no reliable landmarks to distinguish between these structures. All subfield markings were done by a single rater blinded to the diagnosis using rview (http://www.colin-studholme.net/software/software.html) which allows the display of all three orientations simultaneously and thus increases the marking accuracy (as evidenced by a higher ICC compared to Mueller et al., 2007 for which EditBrain was used for subfield marking). Five MCI and five AD and 10 control subjects were randomly selected from the study population and marked twice to establish test–retest reliability in subjects with diseased hippocampi. Intraclass correlation coefficients were ≥ 0.9 for all subfields, cf. Table I. The volume of the total hippocampus was determined from the T1 image using the hippocampal masks provided by the FreeSurfer subcortical parcellation routine [Fischl et al., 2002]. All maps were visually checked for accuracy by different, specially trained raters who were blinded to the diagnosis and manually corrected by overlaying the label generated in FreeSurfer onto the T1 image in rview. This procedure generated a map of comparable accuracy as obtained by a manual marking scheme (ICC for manual correction of the Freesurfer labels: 0.9). The ICV was determined using the BET program (FMRIB Image Analysis Group, Oxford University, www.fmrib.ox.ac.uk/fsl). The resulting skull stripped imaged was checked by overlaying it onto the image with skull to ensure that all extracranial and skull structures were removed and all intracranial structures fully preserved.

Statistical Analysis

For statistical analysis, left and right volumes of each subject were combined. Multiple linear regression analyses with subfield, respectively hippocampal volume as dependent and age, gender, group (control, MCI, AD), and ICV as independent variables were used to identify volumes with significant disease group effects. Significant group effects were then further

explored using ANOVA tests and Tukey post-hoc analyses ($P < 0.05$). Z-scores were calculated to provide a measure of the severity of volume loss in each subfield. To identify those subfield volumes which distinguished best between disease groups, a stepwise linear discriminant analysis (forward, probability to enter $P < 0.05$) with disease group as dependent and subfield and hippocampal volume as independent variables was performed; age and ICV were forced to be in the model. The discriminant analysis was done for each comparison separately, i.e. controls vs. MCI, controls vs. AD, and AD vs. MCI. This analysis was restricted to subfields which had shown a significant group effect in the multiple regression analysis. Finally, using the error estimates from the ANOVA tests, the statistical power to detect a difference at a significance level alpha = 0.05 between controls and AD and controls and MCI for each subfield and total hippocampal volume were calculated. All statistical analyses were done in JMP7 (SAS Institute).

RESULTS

Pattern of Subfield Volume Loss

Multiple regression analysis showed significant effects for disease group for ERC ($P = 0.004$), subiculum ($P = 0.003$), CA1 ($P = 0.0001$), CA1-2 transition ($P < 0.0001$), and hippocampal volume ($P = 0.0005$) but not for CA3&DG. There was a significant negative effect of age on CA1 ($P = 0.0067$) consistent with the findings of our previous study in normal aging [Mueller et al., 2007]. The age effect on CA1 persisted when subjects who were part both studies were excluded from the analysis. Post-hoc analyses (cf Tables II and III) showed that compared to controls AD had significantly reduced ERC, subiculum, CA1, CA1-2 transition, and hippocampal volumes, whereas CA3&DG volumes were not different. CA1 had the smallest *z*-score indicating that this was the subfield with the most pronounced volume loss. In contrast, the atrophy was more restricted in MCI who compared to controls showed significant volume losses in CA1-2 transition but not in ERC, CA1, subiculum, CA3&DG, or total hippocampal volume. There were no significant differences between AD and MCI and the volumes of the MCI group tended to be in-between the volumes of controls and AD with the exception of the CA1-2 transition volume which was close to the volume measured in AD.

Discriminant and Power Analyses

Stepwise linear discriminant analysis showed that CA1 and CA1-2 transition distinguished best between AD and controls (Wilks' Lambda 0.72, $P = 0.0002$, % misclassified: 22.5%, area under the curve (AUC): 0.84, sensitivity/specificity: 0.83/0.75). The volumes of ERC, subiculum, and total hippocampal volume did not fulfill the criteria to enter the stepwise discriminant analysis despite being significantly smaller in the direct comparison AD vs. controls. CA1-2 transition alone discriminated best between MCI and controls (Wilks' Lambda 0.75, $P = 0.0001$, cf. Table IV) and subiculum best between AD and MCI (Wilks' Lambda 0.76, $P = 0.0225$, % misclassified: 26.3%, AUC: 0.78; sensitivity/ specificity: 0.67/0.8). The results of the discriminant analysis for the other subfields and total hippocampal volume and the results of the power analysis are listed in Table IV.

DISCUSSION

There were two main findings of this study: (1) Hippocampal volume loss in AD is not diffuse but affects some subfields more than others. In MCI the volume loss is most prominent in CA1-2 transition, in AD CA1, ERC, subiculum, and total hippocampal volume are affected as well while CA3&DG is spared. (2) CA1-2 transition was the region which distinguished best between MCI and controls and had the highest statistical power to detect differences between these two groups. CA1-2 transition and CA1 discriminated best between AD and controls but their power to distinguish between the two was not different from the power of total

hippocampal volume. These findings indicate that subfield measurements might be a more sensitive way to detect MCI than whole hippocampus measurements but do not provide an advantage over total hippocampal volume for the detection of AD.

The first finding of this study was that hippocampal volume loss in the AD disease process is regionally selective. In AD, the most prominent volume losses were found in CA1-2 transition, CA1, subiculum, and ERC, while in MCI only CA1-2 transition was significantly affected. Although there is general agreement that CA1 is severely affected in AD, there is some controversy if CA2 is affected as well [West et al., 1994; Zarow et al., 2005; Bobinski et al., 1998; Fukutani et al., 1995, 2000]. Because of this and considering the limitations of the CA1-2 transition label (cf. methods section), we assume that the volume loss in this region is driven by volume loss in the dorsal aspect of CA1 rather than in CA2 itself. This suggests that the dorsal CA1 sector is relatively early affected by the AD disease process when the volume loss in ventral part is still relatively mild. In the AD stage, the atrophic changes in CA1 become more pronounced and the disease also spreads to the subiculum that results in a significant loss of total hippocampal volume. This distribution of hippocampal volume loss in the AD disease process is different from the distribution found in normal aging which was restricted to CA1 and did not affect CA1-2 transition and subiculum [Mueller et al., 2007]. The pattern of hippocampal volume loss is also in good agreement with findings of neuroimaging studies at 1.5 T using surface mapping and shape analysis to make inferences about pattern of hippocampal subfield volume loss in AD [Apostolova et al., 2006a, b; Csernansky et al., 2005; Wang et al., 2006].

More importantly though, the atrophy pattern is in good agreement with histopathological studies that consistently show the most prominent neuronal loss or loss of synaptic density in CA1, subiculum and ERC in subjects diagnosed with AD and milder neuron loss mostly restricted to CA1 in subjects suffering from MCI. For example, Fukutani et al. [1995] analyzed the relationship between neurofibrillary tangles (NFT) and unaffected neurons in CA1–4, subiculum, and ERC in six controls and six AD and found significantly increased numbers of NFT in all subfields and decreased numbers of unaffected neurons in CA1, subiculum, and ERC in AD compared to controls. Rössler et al. [2002] studied the relationship between Braak stage and neuron loss in hippocampal subfields in 28 subjects. Compared to stage I, neuron count in CA1 was reduced by 33% in stage IV and by 51% in stage V. The subiculum only became affected in stage V (22% neuron loss). West et al. [1994] assessed neuron counts in the dentate gyrus, CA2/3 and CA1 in seven AD and 19 healthy controls and found the most distinctive cell loss in CA1 (−68%) and less severe losses in subiculum (−47%) and hilus (−25%). The fact that the patterns of regional volume loss found in this neuroimaging study closely resemble the patterns of neuron loss and reduction of synaptic density described in those neuropathological studies, suggests that these volumetric measurements reflect those histopathological changes.

In contrast to CA1, CA1-2 transition, and subiculum, CA3&DG volumes were preserved in MCI and AD. Histopathological studies describe a mild to moderate neuron loss in the dentate gyrus in AD [Simic et al., 1997; Scheff et al., 2006; West et al., 1994]. The dentate gyrus (DG) is part of the polysynaptic intrahippocampal pathway and receives direct excitatory input from the ERC [Duvernoy, 2005]. The ERC is usually early affected in the AD process and showed also in this study a significant volume loss in AD subjects. Therefore, mild atrophic changes in the DG due to deafferentation would have been expected at least in AD. There are two possible explanations why such changes were not found in this study. The most important reason is probably that the DG had to be marked together with CA3. Since CA3 is relatively well preserved in AD, it is possible that it overshadowed subtle effects in DG. Furthermore, although fulfilling the criteria for AD, most of the AD subjects in this study suffered from mild

AD (mean MMSE 21.6) while subjects in autopsy studies tend to suffer from more advanced AD with more pronounced atrophy,

The second finding was that CA1-2 transition volume loss was shown to be a very good measure to distinguish between MCI and controls and together with CA1 between AD and controls. In contrast, total hippocampal volume, which is commonly considered to be the most robust structural imaging marker for AD and MCI, had a comparatively low sensitivity in this study (cf. Table IV) compared to the sensitivity values for the hippocampus reported in the literature which are between 0.7 and 0.85 [Coliot et al., 2008;Kantarci et al. 2002]. This was particularly obvious in AD in whom the sensitivity of the total hippocampal volume was lower than in MCI. There are several possible explanations for this finding. One is the relatively small sample size of AD subjects in this study compared to other studies. Furthermore, the range of MMSE scores in the AD group is relatively large (11–29) indicating that the AD group is heterogeneous regarding disease severity. Finally, the total hippocampal volume has a larger standard deviation in AD than in the two other groups which reduces its ability to correctly classify AD subjects. Seen in the context of the larger range of MMSE scores in AD, the larger standard deviation of the total hippocampal volume is in good agreement with AD group being heterogeneous and containing very mild and more advanced cases. CA1 and CA1-2 transition volumes are less affected by this heterogeneity because both are atrophied in the early and late stages of the disease while the total hippocampal volume contains additional subfields which are not (CA3&DG) or only mildly (Sub) affected in the early stages but develop marked atrophy in the later stages [Rössler et al., 2002].

Those MCI who were misidentified by CA1-2 transition volume loss tended to be younger and less impaired than their correctly identified counterparts (misclassified MCI vs. correctly classified MCI: mean age 68.3 vs. 74.7 years, mean MMSE 29.0 vs. 27.8). This could suggest that they were in an earlier stage of AD than the correctly identified MCI. AD who where misclassified by CA1 and CA1-2 transition volumes were also younger but similarly impaired compared to the correctly identified AD (misclassified AD vs. correctly classified AD: mean age: 66.7 vs. 69.6 years, mean MMSE 21.5 vs. 22.0). This could suggest an earlier onset and thus eventually an atypical presentation of AD or even a different form of dementia and further supports the observation that the AD group was more heterogeneous. However, CA1-2 transition volume loss also incorrectly classified 23% of the controls as MCI and CA1 and CA1-2 transition classified 25% of the controls as AD. Longitudinal studies correlating imaging findings with cognitive changes over time will be necessary to determine if such controls are at an increased risk to develop MCI or if they represent true false positive cases.

Although AD had significantly smaller total hippocampal volumes than controls, total hippocampal volume did not reach significance in the stepwise discriminant analysis after CA1 and CA1-2 transition were included. The same was true for the ERC in MCI and controls although ERC and hippocampus have been shown to be a good measure to discriminate between these groups by other studies [Devanand et al., 2007; Pennanen et al., 2004; Xu et al., 2000]. One reason for the discrepancy regarding ERC might be that we employed a different marking strategy, i.e. ERC in our study was marked on a fixed number of slices while those previous studies determined the number of slices for ERC marking on anatomical landmarks. Therefore, in our marking strategy ERC volume loss is mostly determined by ERC gray matter thinning, while previous studies measured ERC volume loss as a combination of ERC gray matter thinning and overall volume loss of medial temporal structures (lower number of slices on which ERC is marked). Another reason, which also explains the discrepancy regarding the hippocampus, might be that the sample sizes of AD and MCI patients in these studies were larger than in our study and thus the power to detect differences between groups using these measures was greater. In our sample the power to detect a significant difference between controls and AD was 0.98 for total hippocampal volume compared to 0.99 for CA1 and CA1-2

transition, i.e. was practically the same for all three measures but provided CA1 and CA1-2 transition a small advantage over the hippocampus to enter in the stepwise discriminant analysis. This was different for subjects suffering from MCI and controls. The power to detect a difference between those two groups was 0.35 for total hippocampus and 0.28 for ERC but 0.97 for CA1-2 transition. These findings suggest that subfield measurements might be superior to total hippocampal volumetry for the detection of preclinical AD/MCI but provide no advantage over total hippocampal volume in AD.

This study has limitations: (1) The sample size was small although significant findings were obtained. It is necessary to validate the findings in a larger, separate study. On the basis of the current findings, it seems likely that in a larger sample a combination of subfields, e.g. CA1-2 transition and CA1 or CA1-2 transition and ERC will be more powerful to distinguish MCI from controls than CA1-2 transition alone. (2) The study was cross-sectional and we cannot exclude that some of the misclassified controls were in the early stages of AD or some MCI might remain stable or not progress to AD but other dementia types. Follow-up studies are planned. (3) The patients were referred from different memory clinics which although adhering to the same general concept for the diagnosis of MCI and AD (clinical and neuropsychologic evaluation, consensus conference within clinic) use slightly different evaluation procedures. This might have added to the diversity of the MCI and AD groups. (4) Hippocampal subfields were only marked in a relatively small region of the anterior hippocampus. Therefore, we cannot exclude that we missed effects with a regional preference. (5) Although the subfields marking strategy used in this article shows a good correspondence with hippocampal subfields in histopathological samples, it will be necessary to validate the subfield marking strategy in a direct histopathology, imaging correlation study. (6) This technique for subfield volumetry requires a high resolution image which reliably depicts details of the internal structure of the hippocampus, i.e. an image of good quality. This might limit the applicability of this method to severely cognitively impaired and hence noncompliant subjects or subjects suffering from diseases which destroy the internal structure of the hippocampus.

In conclusion, these initial findings suggest that normal aging and AD even in its earliest stages are associated with a distinct pattern of atrophy in the hippocampus, i.e. aging with volume loss in CA1 and MCI with volume loss in CA1-2 transition. Volume loss in CA1-2 transition was superior to total hippocampal volume for discrimination between subjects diagnosed with MCI and controls. Therefore, we conclude that subfield measurements might be a more sensitive way to detect MCI and early AD than measurements of the whole hippocampus.

Acknowledgments

Contract grant sponsor: National Institutes of Health; Contract grant numbers: RO1 AG010897, P01 AG12435.

REFERENCES

Adachi M, Kawakatsu S, Hosoya T, Otani K, Honma T, Shibata A, Sugai Y. Morphology of the inner structure of the hippocampal formation in Alzheimer's Disease. Am J Neuroradiol 2003;24:1575–1581. [PubMed: 13679273]

Apostolova LG, Dutton RA, Dinov ID, Hayashi KM, Toga AW, Cummings JL, Thompson PM. Conversion of mild cognitive impairment to Alzheimer Disease predicted by hippocampal atrophy maps. Arch Neurol 2006;64:693–699. [PubMed: 16682538]

Apostolova LG, Dinov ID, Dutton RA, Hayashi KM, Toga AW, Cummings JL, Thompson PM. 3D comparison of hippocampal atrophy in amnestic mild cognitive impairment and Alzheimer's disease. Brain 2006;129:2867–2873. [PubMed: 17018552]

Bobinski M, de Leon MJ, Tarnawski M, Wegiel J, Bobinski M, Reisberg B, Miller DC, Wisniewski HM. Neuronal and volume loss in CA1 of the hippocampal formation uniquely predicst duration and severity of Alzheimer's disease. Brain Res 1998;805:267–269. [PubMed: 9733982]

Csernansky JG, Wang L, Sank J, Miller JP, Gado M, McKeel D, Miller MI, Morris JC. Preclinical detection of Alzheimer's disease: Hippocampal shape and volume predict dementia onset in the elderly. Neuroimage 2005;25:783–792. [PubMed: 15808979]

Devanand DP, Pradhaban G, Liu X, Khandji A, De Santi S, Sequal S, Rusinek H, Pelton GH, Honig LS, Mayeux R, Stern Y, Tabert MH, de Leon MJ. Hippocampal and entorhinal atrophy in mild cognitive impairment: Prediction of Alzheimer disease. Neurology 2007;68:828–836. [PubMed: 17353470]

De Vita E, Thomas DL, Roberts S, Parkes HG, Turner R, Kinchesh P, Shmueli K, Yousry TA, Ordidge RJ. High resolution MRI of the brain at 4.7 Tesla using fast spin echo imaging. Br J Radiol 2003;76:631–637. [PubMed: 14500278]

Duvernoy, HM. Functional Anatomy, Vascularization and Serial Sections with MRI. 3rd ed.. Berlin: Springer Verlag; 2005.

Coliot O, Chételat G, Chupin M, Desgranges B, Magnin B, Benali H, Dubois B, Garnero L, Eustache F, Lehéricy S. Discrimination between Alzheimer's disease, mild cognitive impairment, and normal aging by using automated segmentation of the hippocampus. Radiology 2008;248:194–201. [PubMed: 18458242]

Eriksson SH, Thom M, Batlett PA, Symms MR, McEvoy AW, Sisodiya SM, Duncan JS. Propeller MRI visualizes detailed pathology of hippocampal sclerosis. Epilepsia 2008;49:33–39. [PubMed: 17877734]

Fischl B, Salat DH, Busa E, Albert M, Dieterich M, Halsegrove C, van der Kouwe A, Killiany R, Kennedy D, Klavenes S, Montillo A, Makris N, Rosen B, Dale AM. Whole brain segmentation: automated labeling of neuroanatomical structures in the human brain. Neuron 2002;33:341–355. [PubMed: 11832223]

Fukutani Y, Kobayashi K, Nakamura I, Watanabe K, Isaki K, Cairns NJ. Neurons, intracellular and extracellular neurofibrillary tangles in subdivisions of the hippocampal cortex in normal ageing and Alzheimer's disease. Neurosci Lett 1995;200:57–60. [PubMed: 8584267]

Fukutani Y, Cairns NJ, Shiozawa M, Sasaki K, Sudo S, Isaki K, Lantos PL. Neuronal loss and neurofirbrillary degeneration in the hippocampal cortex in late-onset sporadic Alzheimer's disease. Psych Clin Neurosci 2000;54:523–529.

Kantarci K, Xu Y, Shiung MM, O'Brien PC, Cha RH, Smith GE, Ivnik RJ, Boeve BF, Edland SD, Kokmen E, Tangalos EG, Petersen RC, Jack CR. Comparative diagnostic utility of different MR modalities in mild cognitive impairment and Alzheimer's disease. Dement Geriatr Cogn Disord 2002;14:198–207. [PubMed: 12411762]

Kesner RP, Hopkins RO. Mnemonic functions of the hippocampus: A comparison between animals and humans. Biol Psychol 2006;73:3–18. [PubMed: 16473455]

Lucassen PJ, Heine VM, Muller MB, van der Beek EM, Wiegant VM, De Kloet ER, Joels M, Fuchs E, Swaab DF, Czeh B. Stress, depression and hippocampal apoptosis. CNS Neurol Disord Drug Targets 2006;5:531–546. [PubMed: 17073656]

Mueller SG, Stables L, Du AT, Schuff N, Truran D, Cashdollar N, Weiner MW. Measurements of hippocampal subfields and age related changes with high resolution MRI at 4T. Neurobiol Aging 2007;28:719–726. [PubMed: 16713659]

Pennanen C, Kivipelto M, Tuomainen S, Hartikainen P, Haenninen T, Laakso MP, Hallikainen M, Vanhanen M, Nissinen A, Helkala EL, Vainio P, Vanninen R, Partanen K, Soininen H. Hippocampus and entorhinal cortex in mild cognitive impairment and early AD. Neurobiol Aging 2004;25:303–310. [PubMed: 15123335]

Petersen RC, Smith GE, Waring SC, Ivnik RJ, Tangalos EG, Kokmen E. Mild cognitive impairment, clinical characterization and outcome. Arch Neurol 1999;56:303–308. [PubMed: 10190820]

Rolls ET, Kesner RP. A computational theory of hippocampal function and empirical tests of the theory. Prog Neurobiol 2006;79:1–48. [PubMed: 16781044]

Rössler M, Zarski M, Bohl J, Ohm TG. Stage dependent and sector specific neuronal loss in hippocampus during Alzheimer's disease. Acta Neuropathol 2002;103:363–369. [PubMed: 11904756]

Simic G, Kostovic I, Winblad B, Bogdanovic N. Volume and number of neurons of the human hippocampal formation in normal aging and Alzheimer's disease. J Comp Neurol 1997;379:482–494. [PubMed: 9067838]

Small SA, Chawla MK, Buoncore M, Rapp PR, Barnes CA. Imaging correlates of brain function in monkeys and rats isolates a hippocampal subregion differentially vulnerable to aging. Proc Natl Acad Sci USA 2004;101:7181–7186. [PubMed: 15118105]

Scheff SW, Price DA, Schmitt FA, Musfson EJ. Hippocampal synaptic loss in early Alzheimer's disease and mild cognitive impairment. Neurobiol Aging 2006;27:1372–1384. [PubMed: 16289476]

Thomas DL, De Vita E, Roberts S, Turner R, Yousry TA, Ordidge RJ. High resolution fast spin echo imaging of the human brain at 4.7T: Implementation and sequence characteristics. Magn Reson Med 2004;51:1254–1264. [PubMed: 15170847]

Wang L, Miller JP, Gado MH, McKeel DW, Rothermich M, Miller MI, Morris JC, Csernansky JG. Abnromalities of hippocampal surface structure in very mild dementia of the Alzheimer type. Neuroimage 2006;30:52–60. [PubMed: 16243546]

West MJ, Coleman PD, Flood DG, Troncoso JC. Differences in the pattern of hippocampal neuronal loss in normal ageing and Alzheimer's disease. Lancet 1994;344:769–772. [PubMed: 7916070]

West MJ, Kawas CH, Stewart WF, Rudiw GL, Troncoso JC. Hippocampal neurons in pre-clinical Alzheimer's disease. Neurobiol Aging 2004;25:1205–1212. [PubMed: 15312966]

Xu Y, Jack CR, O'Brien PC, Kokmen E, Smith GE, Ivnik RJ, Boeve BF, Tangalos RG, Petersen RC. Usefulness of MRI measures of entorhinal cortex versus hippocampus in AD. Neurology 2000;54:1760–1767. [PubMed: 10802781]

Zarow C, Vinters HV, Ellis WG, Weiner MW, Mungas D, White L, Chui HC. Correlates of hippocampal neuron number in Alzheimer's disease and ischemic vascular dementia. Ann Neurol 2005;57:896–903. [PubMed: 15929035]

Zeineh MM, Engel SA, Bookheimer SY. Application of cortical unfolding techniques to functional MRI of the human hippocampal region. Neuroimage 2000;11:668–683. [PubMed: 10860795]

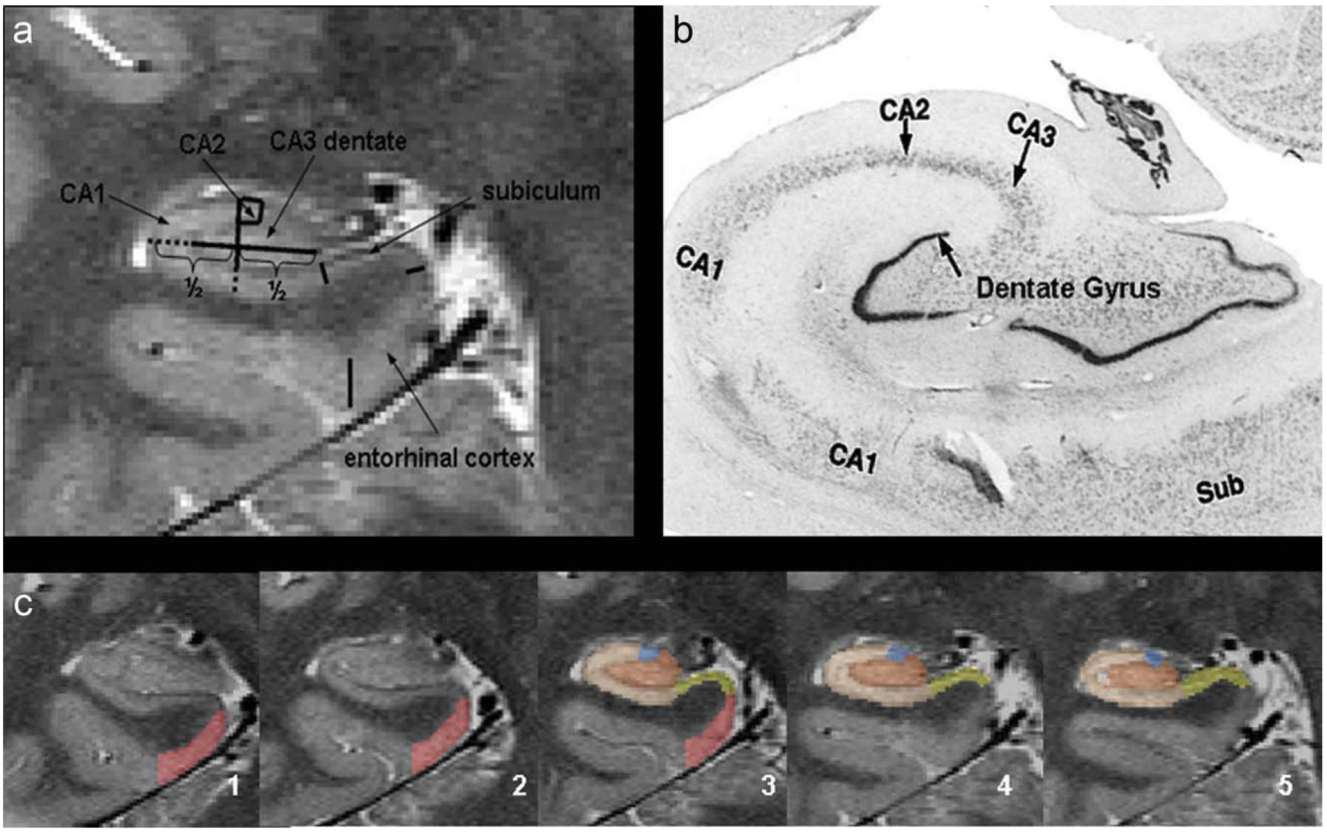

Figure 1.

(**a**) Parcellation scheme used for manual marking of subfields. As it is not possible to identify individual hippocampal layers at 4 Tesla, the scheme was based on reliably recognizable anatomical landmarks even though this resulted in a part of the prosubiculum and subiculum proper being counted towards the CA1 sector. ERC, entorhinal cortex; CA1-2, CA1–CA2 transition zone (cf methods in text); CA3&DG, CA3 and dentate gyrus. (**b**) Histological preparation of hippocampal subfields, arrow, dentate gyrus. (**c**) Typical example of hippocampal subfield markings. No 1 is the most anterior slice, No. 5 the most posterior slice. No. 3 is referred to in the text as “starting” slice. Red, ERC; yellow subiculum; beige; CA1 blue; CA1-2 transition; maroon, CA3&DG. [Color figure can be viewed in the online issue, which is available at wileyonlinelibrary.com.]

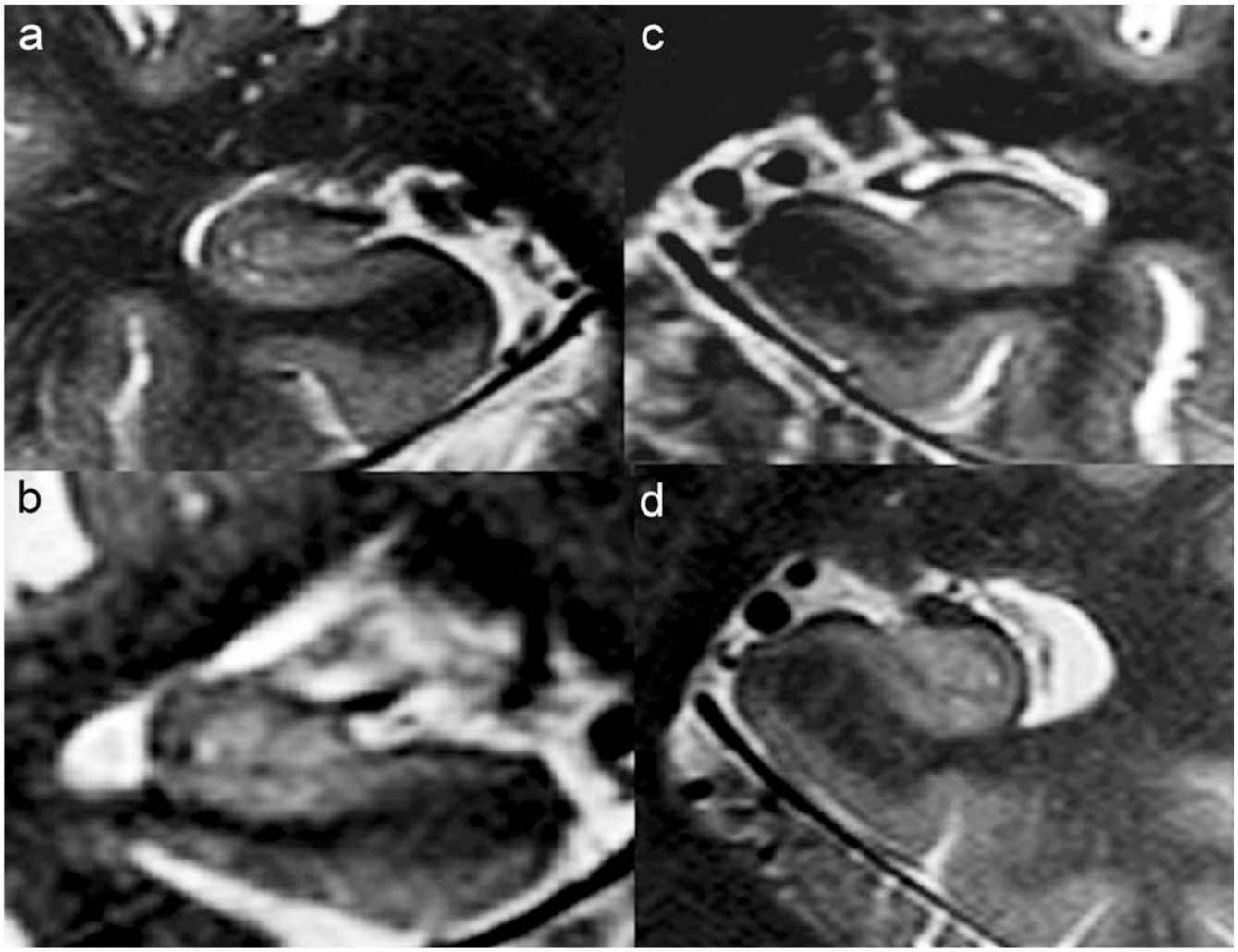

Figure 2.

(**a**) Hippocampal formation of a 78-year-old cognitively nonimpaired man, MMSE 30. The thickness of the dorsal aspect of CA1/CA2 is similar to the thickness of the ventral aspect of CA1. (**b**) Hippocampal formation of a 56 years old female patient with AD, MMSE 12. The hypointense line in AD subjects is less intense than in the control subject but still clearly discernible. (**c**) Hippocampal formation of a 58-year-old male patient with AD, MMSE 24. (**d**) Hippocampal formation of a 71-year-old female MCI patient, MMSE 30. The thickness of the dorsal aspect of CA1/CA2 is reduced compared to the thickness of the ventral aspect of CA1.

TABLE I

Subfield measurement reliability in elderly controls and impaired subjects (AD and MCI)

	Controls (*N* = 10)		AD and MCI (*N* = 10; 5 AD, 5 MCI)	
Subfield	**ICC**	**% Mean volume difference and (range)**	**ICC**	**% Mean volume difference and (range)**
ERC	0.95	5.0 (1.0–10.43)	0.98	4.3 (0–8.3)
Subiculum	0.95	5.0 (0–14.3)	0.97	1.8 (0–6.0)
CA1	0.96	3.5 (1–8.8)	0.97	2.2 (0–4.0)
CA1-2 Transition	0.90	4.8 (0–14.7)	0.90	1.3 (0–12.5)
CA3 & DG	0.96	4.5 (0–7.6)	0.97	2.5 (0–9.2)

TABLE II

Mean and standard deviation of subfield and total hippocampal volumes in mm^3

	Control (n = 53)	MCI (n = 20)	AD (n = 18)
ERC	190.7 ± 54.4	167.4 ± 44.3	144.4 ± 48.3*
Subiculum	190.9 ± 37.8	184.6 ± 31.5	154.7 ± 45.1*
CA1	325.7 ± 48.3	296.9 ± 43.5	271.1 ± 58.0*
CA1-2 transition	19.33 ± 5.4	14.8 ± 2.5*	14.0 ± 3.4*
CA3 & DG	225.6 ± 40.7	230.7 ± 32.1	225.7 ± 49.7
Total hippocampus	5487.6 ± 770.7	5123.2 ± 752.0	4615.9 ± 1182.5*

ERC, entorhinal cortex; CA1-2 transition, CA1–CA2 transition zone (definition see text); CA3 & DG, CA3 and CA4 together with dentate gyrus.

*$P < 0.05$ compared to controls, raw volumes, i.e. not corrected for age of ICV.

TABLE III

Mean and standard deviation of subfield and total hippocampal *z*-scores in AD and MCI

	MCI (*n* = 20)	**AD (*n* = 18)**
ERC	−0.48 ± 0.90	−0.90 ± 0.87
Subiculum	−0.26 ± 1.0	−1.02 ± 1.28
CA1	−0.76 ± 1.0	−1.29 ± 1.28
CA1-2 transition	−0.91 ± 0.50	−1.07 ± 0.58
CA3 & DG	−0.01 ± 0.93	−0.15 ± 1.11
Total hippocampus	−0.65 ± 1.28	−1.38 ± 1.67

The scores were calculated using the following formula: *z*-score = (norm subfield$_{subject}$ − mean norm subfield$_{controls}$)/SD norm subfield$_{controls}$ norm subfield = raw subfield volume normalized to intracranial head volume.

TABLE IV

Results of discriminant and power analysis

	Amnestic MCI vs. controls				AD vs. controls			
	ROC AUC	**% MC**	**Sens/Spec**	**Power**	**ROC AUC**	**% MC**	**Sens/Spec**	**Power**
ERC	0.74	30.1	0.75/0.68	0.28	0.78	35.2	0.72/0.62	0.90
Subiculum	0.72	37.0	0.70/0.60	0.12	0.75	25.3	0.72/0.75	0.91
CA1	0.74	28.7	0.75/0.70	0.51	0.80	30.0	0.67/0.72	0.99
CA1-2 transition	0.83	20.5	0.85/0.77	0.97	0.81	30.0	0.72/0.70	0.98
Total hippocampus	0.72	31.5	0.70/0.68	0.35	0.75	28.7	0.61/0.75	0.98

% MC, percentage of subjects misclassified; Sens/Spec, sensitivity/specificity, AUC, area under the curve of the receiver operating characteristic graphic (ROC); Power, power to the detect a difference between subjects diagnosed with MCI and controls (MCI), respectively, AD and controls (AD) at the significance level alpha = 0.05.

Please see text for ROC and sensitivity/specificity of CA1 in combination with CA1-2 transition to discriminate between AD and controls.